Design and Fabrication of a Multi-electrode Array for Spinal Cord Epidural Stimulation

Chih-Wei Chang, Yi-Kai Lo, Parag Gad, Reggie Edgerton and Wentai Liu

***Abstract*—A detailed design, fabrication, characterization and test of a flexible multi-site platinum/polyimide based electrode array for electrical epidural stimulation in spinal cord prosthesis is described in this paper. Carefully designed 8.4 µm-thick structure fabrication flow achieves an electrode surface modification with 3.8 times enhanced effective surface area without extra process needed. Measured impedance and phase of two type of electrodes are 2.35±0.21 KΩ and 2.10±0.11 KΩ, -34.25±8.07° and -27.71±8.27° at 1K Hz, respectively. The fabricated arrays were then *in-vitro* tested by a multichannel neural stimulation system in physiological saline to validate the capability for electrical stimulation. The measured channel isolation on adjacent electrode is about -34dB. Randles cell model was used to investigate the charging waveforms, the model parameters were then extracted by various methods. The measured charge transfer resistance, double layer capacitance, and solution resistance are 1.9 KΩ, 220 nF and 15 KΩ, respectively. The results show that the fabricated array is applicable for electrical stimulation with well characterized parameters. Combined with a multichannel stimulator, this system provides a full solution for versatile neural stimulation applications.**

I. Introduction

Recovery of locomotion from permanent paralysis caused by spinal cord injuries (SCI) is one of the biggest topics in spinal cord prosthesis. It is known that networks of neurons in the lumbosacral spinal cord retain an intrinsic capability to oscillate and generate coordinated rhythmic motor outputs [1]. Circuits underlying such rhythmic and oscillatory outputs are commonly referred as central pattern generators (CPGs) [2]. Studies demonstrated that the animals can regain motor ability from the plasticity of spinal cord [3], including stepping and standing by stimulating the CPGs without the control from brain [4]. To provide the stimulus patterns into the spinal cord, various electrode arrays were developed for such proposes with specificities [4-6]. Electrodes for spinal cord stimulation should also provide enough mechanical flexibility and durability to against the possible movement from animal motions, as well as the selectable/programmable multi-site electrodes to gain the best stimulation parameters.

Research partially supported by grants from California Capital Equity LLC, UC Laboratory Research Fee Program and NSF ERC BMES.

Chih-Wei Chang is with the Department of Bioengineering, UCLA, Los Angeles, CA 90095 USA(phone:424-248-8655;e-mail:cw.chang@ucla.edu).

Yi-Kai Lo is with the Department of Bioengineering, UCLA, Los Angeles, CA 90095 USA (e-mail: yikai.lo@ucla.edu).

Parag Gad is with the Department of Integrative Biology and Physiology, UCLA, Los Angeles, CA 90095 USA (e-mail: paraggad@ucla.edu).

Reggie Edgerton is with the Department of Integrative Biology and Physiology, UCLA, Los Angeles, CA 90095 USA (e-mail: vre@ucla.edu).

Wentai Liu is with the Department of Bioengineering, UCLA, Los Angeles, CA 90095 USA (e-mail: wentai@ucla.edu).

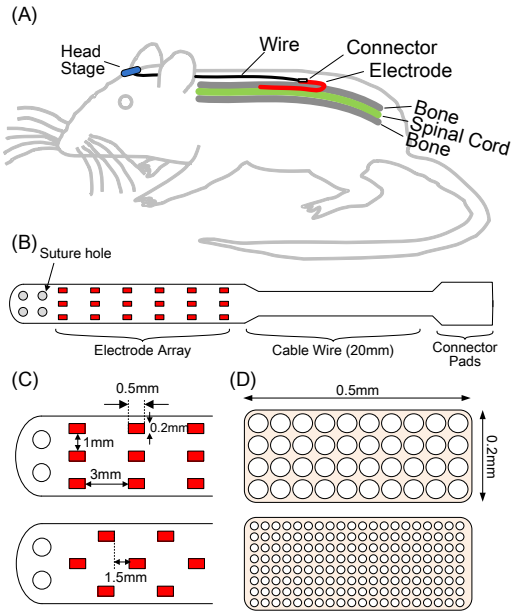

Figure 1. The application target of the implantable spinal cord prosthesis on the rat and the electrode design schematic. Two types of the electrode array design (Upper: regular; lower: interlaced design) and two types of grid window on the electrodes are designed for future experiments.

In this work, we present a flexible multi-site polymer electrode array for epidural spinal cord stimulation. For the selection of the materials, several design features were taken into account. Low stress thin film polyimide was chosen as electrode substrate because of its superior high mechanical strength, low moisture uptake rate, low dielectric constant property with great biocompatibility than other polymers [7]. Platinum/Titanium metal layer was selected for its high stability and biocompatibility. A roughening process was used to increase the effective surface area. This in turn lowered the electrode-electrolyte interface impedance as well as the compliance working voltage to allow the induced electrode to be operated within the water window [8]. Electrode density was taken into consideration when designing the array. Dense arrays provide more stimulus pattern combinations, but similar or unwanted stimulus effect may happen in the neighborhood of the stimulated electrode due to limited stimulus spatial resolution between adjacent electrodes. In-vitro stimulation test of the fabricated array was demonstrated by using a multichannel stimulator in saline solution. This work also presents an electrode-electrolyte modeling via a new time-domain large signal analysis method developed by our group [14]. Detailed design and characterization procedures and results are described in the following sections.

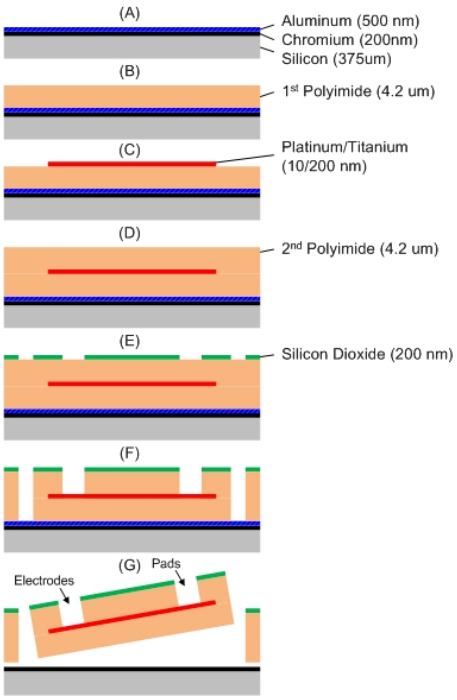

Figure 2. Fabrication process of the flexible polymer electrode array.

II. Electrode Design and Fabrication

Figure 1 illustrates the application goal and electrode designs. As shown in Figure 1 (A) and (B), the electrode array was designed to be placed in the epidura space between dura matter and the upper layer of the vertebrae. Suturing holes are designed on the tip (electrode side) of the array, which allows surgeons to fix the array onto the dura matter by suture. The back-end (connector side) of the electrode array is then surgically placed through the upper spinal cord and connected to lead wires to the headstage via a connector. Two types of the electrode arrangements, regular and interlaced design, and two kinds of grid window design (45 µm and 20µm in diameter) on the electrode are designed for various stimulation combinations in our future animal experiments. Comparing with the normal single electrode opening design [6], the grid window designs are adapted to provide a more uniform stimulus current density and additional protection of the metal from peeling during the large and continuous current stimulation.

Figure 2 describes the fabrication flow of the electrode array. (A) Chromium/Aluminum (200 nm/ 500 nm) layer was deposited by E-beam evaporated deposition (CHA Mark 40) on to a handle wafer. An adhesion promoter (VM-651, HD Microsystems) was applied to create a Si-C bond and provide additional adhesion for the first polyimide layer. (B) A 4.2 µm polyimide (PI-2611, HD Microsystems) was spin-coated onto the wafer, and cured in 350°C for 30 minutes in a nitrogen-controlled oven to form full cross-link in the polyimide. (C) Titanium/Platinum (10nm/ 200 nm) layer was defined and deposited using E-beam evaporated deposition (CHA Mark 40) and a lift-off technique. An oxygen-plasma roughening process was applied to the first polyimide layer for 30 seconds before the Titanium/Platinum deposition to enhance the adhesion performance. (D) Another 4.2 µm polyimide (PI-2611, HD Microsystems) was spin-coated onto

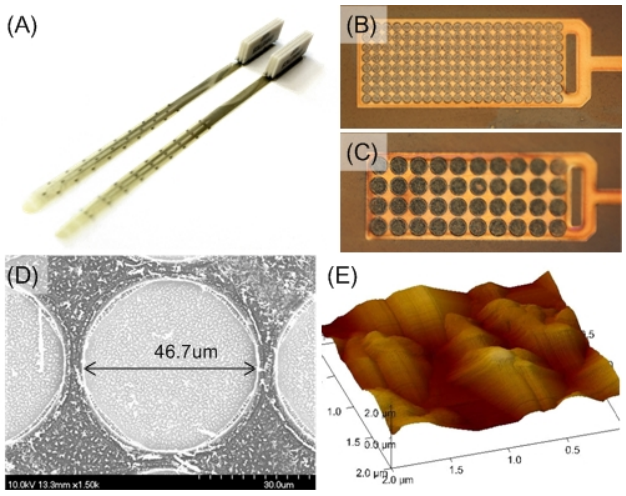

Figure 3. Fabrication results (A) Fabricated electrode arrays soldered with connectors. (B) Electrode with small grid window. (C) Electrode with big grid window. (D) Scanning electron microscopy of a single grid window. (E) Atomic force microscopy.

the wafer, and cured in 350°C for 30 minutes in a nitrogen-controlled oven. (E) A silicon dioxide (200 nm) film was deposited using a DC sputter (Denton Discovery-550) and defined by CHF_3/Ar reactive ion etch (RIE) process using a plasma etcher (Oxford Plasmalab-80 Plus). (F) A pure oxygen plasma process was used to define the array shape as well as exposing the metal layer of electrodes and connector pads. An extra oxygen/CF_4 RIE process was utilized to remove the residual layer composed of the silicon containing active ingredient (a-aminopropyltriethoxysilane) which is caused by the Si-C bond promoter [9]. (G) Finally, the electrode arrays were detached from the handle wafer by anodic metal dissolution in a 10 wt% sodium chloride solution [10]. The anodic metal dissolution process dissolved the aluminum, leaving the chrome on the substrate, thus releasing the polyimide electrode arrays. After the fabrication, surface connectors (Neural Connector, Omnetics) were soldered onto the arrays. Silicone encapsulation (Sylgard 184) was then applied to seal all the soldering parts and cured in a 120°C oven for 20 minutes to fully coagulate.

III. Fabrication Results and Characterization

Figure 3 shows the fabrication results. (A) Fully Packaged arrays. Two types of the electrode arrangement can be seen. (B) Optical microscopy of the electrode with small grid window. (C) Optical microscopy of the electrode with large grid window. Note that the platinum shows a dark color due to the roughened surface. (D) Scanning electron microscopy (SEM) of one single opening of the electrode with large grid window. The measure diameter is 46.7µm, which is slightly bigger than the original design (45µm).

Figure 3 (E) shows the atomic force scanning (AFM) on a 2 µm by 2 µm area of the platinum electrode surface. The scanning was operated under tapping mode. From the AFM measurement result, the platinum film shows a roughened surface rather than a pure flat surface. The curved surface is caused by the fluorine attack on platinum etching [11] during the oxygen/CF_4 RIE process in figure 2 (F). The surface roughness of the platinum surface is 319 nm in root-mean-square (RMS), 266 nm in average and 1716 nm in

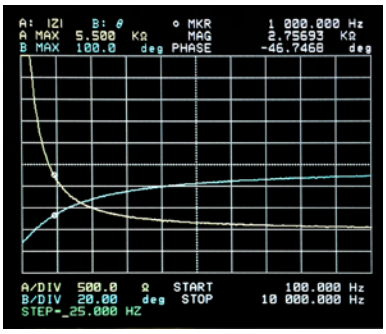

Figure 4. Measured impedance of the fabricated electrode array.

maximum with 15.2 μm^2 effective area, which is 3.8-times larger than the scanning area. According to the literature survey, the double-layer capacitance of the platinum electrode is about 40-80 $\mu F/cm^2$ within the reversible hydrogen electrode (RHE) potential limits [12]. Therefore, the calculated capacitance is around 104.1-208.2 nF.

Figure 4 shows the measured impedance of one of the fabricated in a 0.9 wt% physiological sodium chloride solution through an impedance analyzer (HP 4194A). An Ag/AgCl electrode (P-BMP-1, ALA scientific instruments) was used as the reference electrode. The averaged impedance and phase of the large and small grid electrode are 2.35±0.21 KΩ and 2.10±0.11 KΩ, -34.25±8.07° and -27.71±8.27° at 1K Hz with 10 mV input level, respectively (Tested electrode number = 27 for each type of the electrode).

IV. Stimulation Test by Multichannel Stimulation System

To validate the electrode performance in practical stimulation, the fabricated electrodes were tested using a multichannel current-mode neural stimulator [13] developed by our group with the same physiological saline solution setup as the impedance analysis, as shown in Figure 5. Figure 6 illustrates the Randles cell model of the electrode-electrolyte interface with three elements, which consist of a charge transfer resistance R_{CT}, a double layer, capacitance C_{dl}, and a tissue-solution resistance R_S, respectively.

The stimulation result was displayed in Figure 7. A stimulus biphasic input with 10 µA cathodic/anodic current intensity, 8 ms pulse width and 7 ms inter-pulse delay was injected into to the electrode. A mathematical expression of the voltage waveform is described according to the Randles cell model. At the cathodic rising edge, the input signal can be seen as a very high frequency therefore the C_{dl} becomes a short circuit, all the current will charge the R_S and cause a shape voltage drop. After the evolution comes to the flat cathodic region, the DC current starts to charge the C_{dl} and R_{CT}, which results in an exponential-like waveform. At the cathodic falling edge, the C_{dl} is short again, and discharges the R_S. After entering the flat anodic region, the DC current starts to discharge the C_{dl} and R_{CT} back to the electrode.

Coupling effect was evaluated by injecting stimulus current into an electrode, and recording the coupled stimulus signal from a nearest adjacent electrode. As shown in Figure 8, a maximal electrode voltage of 640 mV in the cathodic phase was induced by a biphasic stimulus current input with 100 µA

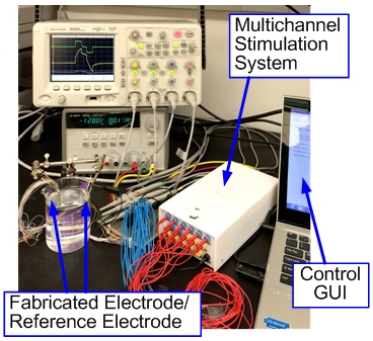

Figure 5 Experiment setup. The fabricated electrode was tested by a multichannel stimulation system controlled by a laptop-based GUI.

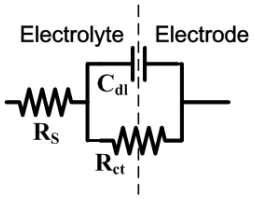

Figure 6 Randles cell model of the electrode-electrolyte interface. R_{CT}: charge transfer resistance; C_{dl}: double layer capacitance; R_S: tissue-solution resistance.

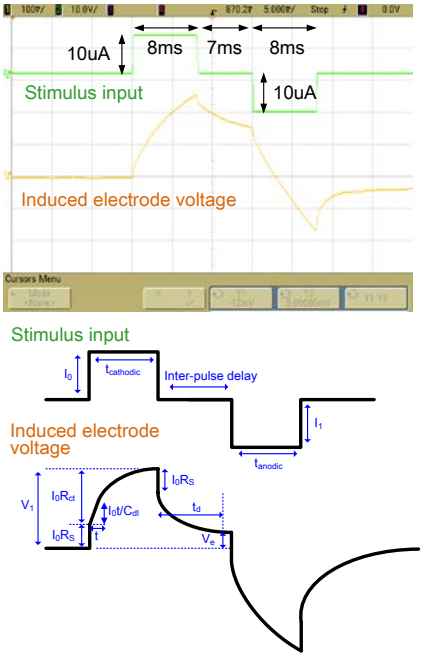

Figure 7 Induced voltage waveform on the electrode during the biphasic current stimulation. A mathematical expression of the voltage waveform is described according to the Randle cell model.

cathodic/anodic current, 1 ms pulse width and 0.8 ms inter-pulse delay. A 7 mV coupled pulse signal with similar waveform as the stimulus signal was simultaneously recorded from a nearest adjacent electrode. The coupled stimulus signal decayed for -39.22 dB, which shows an ignorable coupled stimulus side effect.

To investigate the validity of the electrode model in detail, we used an impedance acquisition technique based on large signal analysis developed in our group [14]. The parameters of

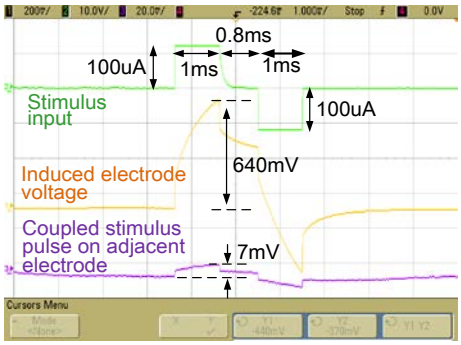

Figure 8. Channel isolation test.

the Randles cell electrode model can be inferred from the pre-determined stimulus parameters, such as pulse width and interpulse delay, and measurement of the resulting transient electrode voltage. The R_S can also be validated by looking into the impedance in very high frequency in Figure 4, which is closed to the calculation result. The calculated double layer capacitance is also similar to the value from AFM result in Section II. Note that another possible way to evaluate the C_{dl} is using the zero on the impedance plot (Figure 4) using R_S:

$$Zero = 1/2\pi C_{dl}\left(R_{CT} \,||\, R_S\right) \quad (1)$$

R_{CT} might be able to be ignored if $R_{CT} >> R_S$. A summarized specification of the fabricated array can be found in Table I.

TABLE I SPECIFICATION SUMMARY

Electrode Materials	Platinum and Polyimide
Array Thickness/ Electrode dimension	8.4 µm/ 0.5 mm x 0.2 mm
Effective Area Factor	3.8
Surface Roughness RMS	319 nm
Impedance@ 1K Hz	2.35±0.21 / 2.10±0.11 KΩ
Phase@ 1K Hz	-34.25±8.07° / -27.71±8.27°
Double Layer Capacitance*	220 nF
Charge Transfer Resistance*	15 KΩ
Tissue Resistance*	1.9 KΩ
Channel Isolation	-39.22 dB

* Tested in 0.9 wt% physiological sodium chloride solution

V. CONCLUSION

A flexible polymer electrode array was designed, fabricated, characterized and in-vitro tested by using a multichannel stimulator in saline solution for the demonstration of electrical spinal cord stimulation. Low stress polyimide with superior mechanical property was used to fit the requirement of spinal cord implant. Various electrode grid window and array arrangements were proposed to enhance the uniformity of the stimulus charge density and the stimulation pattern combinations. The roughened platinum electrode surface yielded a 3.8x effective area which increased the equivalent double layer capacitance and therefore enhanced the charge transfer capability. The electrode transient waveform was investigated using a lumped Randles cell model with a multichannel stimulation system, which allowed us to examine the channel isolation and extract the parameters of the electrode model. The model is further validated by various approaches including the large signal analysis technique, AFM and impedance analyzer. The results show that the fabricated electrode is applicable for electrical stimulation with well characterized performance. Combined with a multichannel stimulator, this array completes a full system solution for various applications.

REFERENCES

[1] S. Grillner, "Biological Pattern Generation: The Cellular and Computational Logic of Networks in Motion," *Neuron,* vol. 52, pp. 751-766, 2006.

[2] G. Courtine, Y. Gerasimenko, R. van den Brand, A. Yew, P. Musienko, H. Zhong, B. Song, Y. Ao, R. M. Ichiyama, I. Lavrov, R. R. Roy, M. V. Sofroniew, and V. R. Edgerton, "Transformation of nonfunctional spinal circuits into functional states after the loss of brain input," *Nature Neuroscience,* vol. 12, pp. 1333-U167, Oct 2009.

[3] I. Lavrov, Y. P. Gerasimenko, R. M. Ichiyama, G. Courtine, H. Zhong, R. R. Roy, and V. R. Edgerton, "Plasticity of Spinal Cord Reflexes After a Complete Transection in Adult Rats: Relationship to Stepping Ability," *Journal of Neurophysiology,* vol. 96, pp. 1699-1710, 2006-09-14 18:42:11 2006.

[4] P. Gad, J. Choe, M. S. Nandra, H. Zhong, R. R. Roy, Y.-C. Tai, and V. R. Edgerton, "Development of a multi-electrode array for spinal cord epidural stimulation to facilitate stepping and standing after a complete spinal cord injury in adult rats," *Journal of Neuroengineering and Rehabilitation,* vol. 10, Jan 21 2013.

[5] M. S. Nandra, I. A. Lavrov, V. R. Edgerton, and T. Yu-Chong, "A parylene-based microelectrode array implant for spinal cord stimulation in rats," in *Micro Electro Mechanical Systems (MEMS), 2011 IEEE 24th International Conference on*, 2011, pp. 1007-1010.

[6] P. N. Gad, C. Jaehoon, K. G. Shah, A. Tooker, V. Tolosa, S. Pannu, G. Garcia-Alias, Z. Hui, Y. Gerasimenko, R. R. Roy, and V. R. Edgerton, "Using in vivo spinally-evoked potentials to assess functional connectivity along the spinal axis," in *Neural Engineering (NER), 2013 6th International IEEE/EMBS Conference on*, 2013, pp. 319-322.

[7] T. Walewyns, N. Reckinger, S. Ryelandt, T. Pardoen, J.-P. Raskin, and L. A. Francis, "Polyimide as a versatile enabling material for microsystems fabrication: surface micromachining and electrodeposited nanowires integration," *Journal of Micromechanics and Microengineering,* vol. 23, Sep 2013.

[8] D. R. Merrill, M. Bikson, and J. G. R. Jefferys, "Electrical stimulation of excitable tissue: design of efficacious and safe protocols," *Journal of Neuroscience Methods,* vol. 141, pp. 171-198, Feb 15 2005.

[9] B. Mimoun, H. T. M. Pham, V. Henneken, and R. Dekker, "Residue-free plasma etching of polyimide coatings for small pitch vias with improved step coverage," *Journal of Vacuum Science & Technology B,* vol. 31, Mar 2013.

[10] M. Datta, "Anodic dissolution of metals at high rates," *IBM Journal of Research and Development,* vol. 37, pp. 207-226, 1993.

[11] J.-S. Maa, H. Ying, and F. Zhang, "Effect of temperature on etch rate of iridium and platinum in CF_4/O_2," *Journal of Vacuum Science & Technology A: Vacuum, Surfaces, and Films,* vol. 19, pp. 1312-1314, 2001.

[12] W. G. Pell, A. Zolfaghari, and B. E. Conway, "Capacitance of the double-layer at polycrystalline Pt electrodes bearing a surface-oxide film," *Journal of Electroanalytical Chemistry,* vol. 532, pp. 13-23, Sep 6 2002.

[13] L. Yi-Kai, C. Kuanfu, P. Gad, and L. Wentai, "A Fully-Integrated High-Compliance Voltage SoC for Epi-Retinal and Neural Prostheses," *Biomedical Circuits and Systems, IEEE Transactions on,* vol. 7, pp. 761-772, 2013.

[14] Yi-Kai Lo, Chih-Wei Chang and Wentai Liu, "Bio-Impedance Acquisition Technique Using Biphasic Current Stimulus Excitation for Implantable Neural Stimulator," *Accepted by IEEE Conf. Eng. Med. Biol. , 2014.*